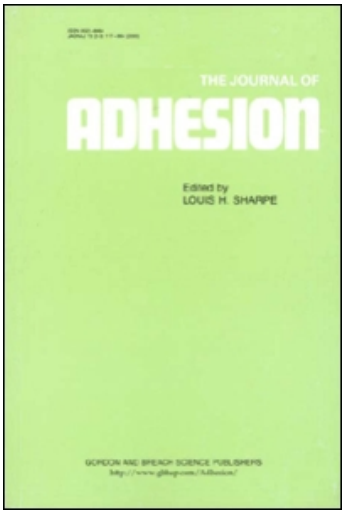

The Journal of Adhesion
Publication details, including instructions for authors and subscription information:
http://www.informaworld.com/smpp/title~content=t713453635

A Model for the Diffusion of Moisture in Adhesive Joints. Part II: Experimental

D. R. Lefebvre[a]; O. A. Dillard[b]; H. F. Brinson[b]
[a] Matls. Engineering Science Dept., Virginia Tech., Blacksburg, VA, U.S.A. [b] Engineering Sci. & Mechanics Dept., Virginia Tech., Blacksburg, VA, U.S.A.

To cite this Article Lefebvre, D. R. , Dillard, O. A. and Brinson, H. F.(1989) 'A Model for the Diffusion of Moisture in Adhesive Joints. Part II: Experimental', The Journal of Adhesion, 27: 1, 19 — 40
To link to this Article: DOI: 10.1080/00218468908050591
URL: http://dx.doi.org/10.1080/00218468908050591

J. Adhesion, 1989, Vol. 27, pp. 19–40
Reprints available directly from the publisher
Photocopying permitted by license only

Printed in the United Kingdom

A Model for the Diffusion of Moisture in Adhesive Joints. Part II: Experimental

D. R. LEFEBVRE

Matls. Engineering Science Dept., Virginia Tech., Blacksburg, VA 24061, U.S.A.

D. A. DILLARD*

Engineering Sci. & Mechanics Dept., Virginia Tech., Blacksburg, VA 24061, U.S.A.

H. F. BRINSON

Engineering Sci. & Mechanics Dept., Virginia Tech., Blacksburg, VA 24061, U.S.A.

(Received December 29, 1987; in final form August 12, 1988)

The concentration dependence and temperature dependence of the diffusion coefficient, as discussed in Part I, are validated with literature data on poly(styrene) and on poly(vinylacetate). The effect on diffusivity, of a uniaxial tensile stress state and of a biaxial tensile stress state, is measured with permeation tests on stretched poly(ethyleneterephthalate) (PET) films. The influence of semi-crystallinity is briefly discussed. Further, diffusivity measurements under a tensile stress state, under a compressive stress state, and under a pure shear stress state are performed on Ultem® polyimide films, using a modified sorption technique. Good agreement between theoretical predictions and experiment is found. Finally, predictions by the solubility model discussed in Part I are compared with data on low density polyethylene and on Ultem polyimide.

KEY WORDS Permeation; sorption; solubility; stress; strain; polymers.

INTRODUCTION

Governing equations for the diffusion of moisture in adhesives and, more generally, for the diffusion of small molecules in polymers, were derived in Part I. A theory for the diffusion coefficient, based on free volume, and a theory for solubility, based on the thermodynamics of mixtures, have been proposed. In Part II, the diffusivity and solubility models are validated, using selected experimental data from the literature as well as data collected by the author. Since the primary goal of this section is to verify transport theories, the polymers studied need not be good adhesives. For the same reason, penetrants other than

* To whom correspondence should be addressed.

moisture can be used. The polymer-sorbent systems studied are; ethylbenzene-poly(styrene), toluene-poly(styrene), toluene-poly(vinylacetate), PET-oxygen, PET-carbon dioxide, PET-water, Ultem poly(imide)-water, and low density poly(ethylene)-carbon dioxide. Only the poly(imide) was selected specifically for this study.

The new contributions are found mainly in the area of stress effects. Two general methods are available for measuring transport properties in mechanically-loaded polymers: permeation and sorption. Data obtained with both techniques will be presented. Most of the literature data featuring stress effects seem to have been obtained by permeation techniques. Permeation techniques, however, are limited to tensile stress states because the permeation membranes cannot be loaded in compression or in shear. (The small membrane thickness results in buckling under those conditions). For this reason, a new modified sorption technique was designed, which permits the study of compressive and shear stress states.

THE TEMPERATURE AND CONCENTRATION DEPENDENCE OF DIFFUSIVITY IN POLY(STYRENE) AND IN POLY(VINYLACETATE) IN THE RUBBERY RANGE

An expression for the temperature, concentration and strain dependence of diffusivity above T_g was derived in Part I. In the absence of any mechanical volumetric strain, as expected in the rubbery state, we found that one should have:

$$D = \frac{D_0}{T_0} T \exp\left\{\frac{B^D}{f_0} \frac{\alpha(T - T_0) + \gamma C^N}{f_0 + \alpha(T - T_0) + \gamma C^N}\right\} \tag{26'}$$

Expression (26') was fitted with diffusion coefficients from experimental data obtained by Vrentas *et al.*[14,27] for the temperature and concentration dependence in the rubbery range. The data were extracted from step-change sorption experiments following a complex procedure discussed in Reference 27. The solute-polymer systems investigated were: ethylbenzene-poly(styrene), toluene-poly(styrene), and toluene-poly(vinylacetate). Each set of data provides diffusion coefficients for a number of concentrations and temperatures.

Expression (26') was fitted to each of the three data sets using a nonlinear least square routine. D was expressed in m^2/sec in order to compare the fitting parameters with the known WLF constants. The resulting parametric curves with the corresponding experimental data for the ethylbenzene-poly(styrene), the toluene-poly(styrene), and the toluene-poly(vinylacetate) systems, are shown in Figures 1, 2 and 3, respectively. By itself, the level of correlation obtained only shows that the mathematical form of Expression (26') is promising. In order to demonstrate the predictive capability of the model, the fitting parameters were compared with the expected constants as given by the free volume theory of Williams, Landel and Ferry. The results are summarized in Table I and II. Within a small error, the obtained values for B^D/f_g, D_g and T_g were correct and were

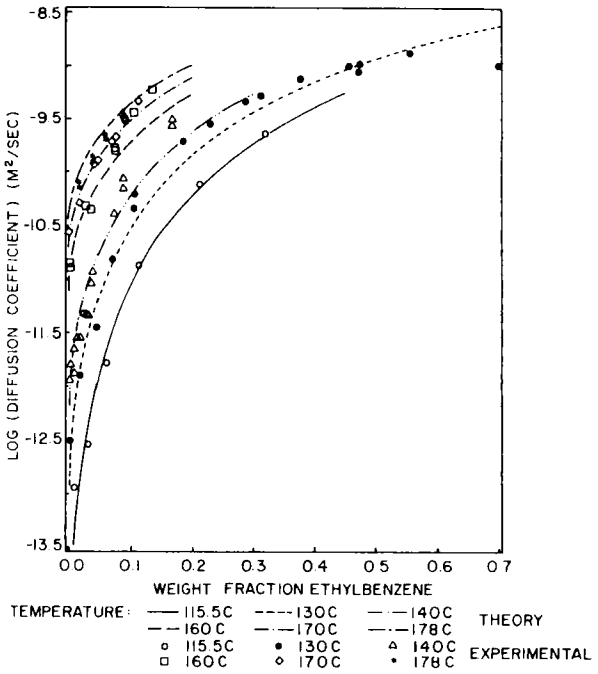

FIGURE 1 Validation for temperature and concentration dependence; ethylbenzene-poly(styrene) system. Data from Vrentas & Duda.[27]

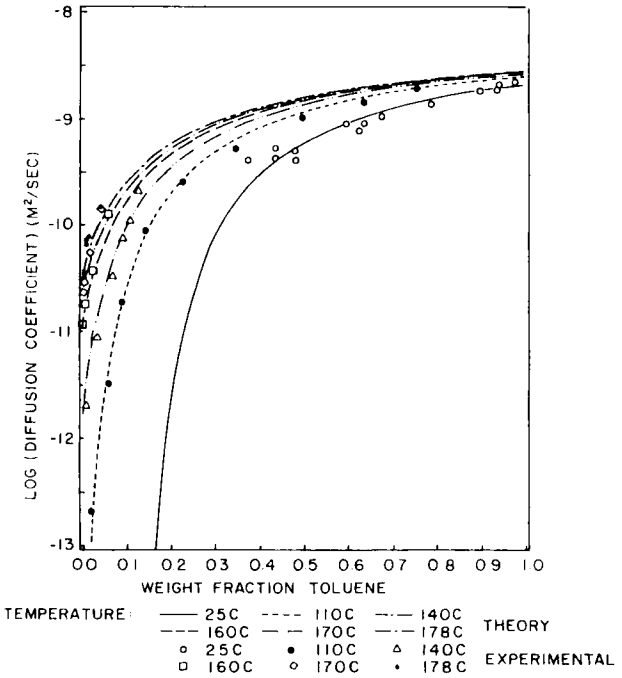

FIGURE 2 Validation for temperature and concentration dependence; toluene-poly(styrene) system. Data from Vrentas & Duda.[27]

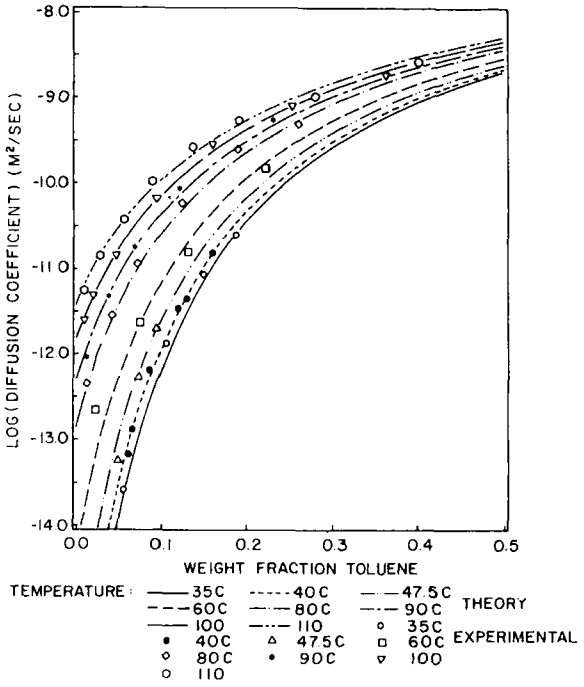

FIGURE 3 Validation for temperature and concentration dependence; toluene-poly(vinylacetate) system. Data from Vrentas & Duda.[27]

TABLE I
Self-diffusion data for poly(styrene)

SELF DIFFUSION DATA FOR POLYSTYRENE:

SOURCE:	log D_g	B^o/f_g	α_g (deg-1)	f_g	T_g (C)	γ	N
PS FERRY'S WLF theory	-	30.30	.00069	0.033	97.	-	-
ETHYLBENZENE - POLYSTYR DIFF DATA BEST FIT	-24.3	17.9	.00255	0.074	80.	0.48	0.61
TOLUENE - POLYSTYR DIFF DATA BEST FIT	-24.6	16.4	.00099	0.014	88.	0.51	0.90

TABLE II
Self-diffusion data for poly(vinylacetate)

SELF DIFFUSION DATA FOR POLYVINYLACETATE:

SOURCE:	$\log D_g$	B^o/f_g	α_g (deg-1)	f_g	T_g (C)	γ	N
PVac FERRY'S WLF theory	-	35.71	.00044	0.028	32.	-	-
TOLUENE - PVac DIFF DATA BEST FIT	-15.5	8.8	.00450	0.319	50.3	2.1	0.91

independent of the nature of the solvent. In addition, the obtained T_g values for the two polymers were quite close to the actual T_g's. The variations in α_g and f_g for polystyrene were disappointing, however.

Since the amount of swelling is so large in the three polymer-solvent systems investigated, our model was, in fact, pushed beyond its expected solvent-mass-fraction range. On a purely theoretical basis, the Vrentas–Duda model would be more appropriate when such high solvent concentrations are found in the polymer. In practice, however, the number of fitting parameters is so large in the Vrentas–Duda model {14 parameters, *versus* 7 in expression (26′)}, that from a purely mathematical point of view, its curve-fitting capability is not improved significantly over that of Expression (26′). We conclude that in the cases investigated, Expression (26′) is a promising phenomenological representation of the temperature and concentration dependence of the diffusion coefficient in the rubbery range. It must be emphasized that this conclusion does not constitute a setback for the Vrentas–Duda model. Rather, it is found that the simplified form given by (26′) can be used provided the data justify such a simplification. Since moisture concentrations in adhesives are relatively low compared to the concentrations encountered in the three systems above, we *a fortiori* expect excellent results in a study of moisture diffusion in adhesives, in a comparable temperature range.

THE STRESS DEPENDENCE OF DIFFUSIVITY IN AMORPHOUS PET AND IN SEMICRYSTALLINE PET

The predictive capability of the Free Volume Theory for stress dependence in a glassy polymer was verified using experimental data collected by the authors of Reference 28. The diffusion of O_2, CO_2 and H_2O through strained Poly(ethylene terephtalate) films and through pressurized PET containers was studied. The measured parameter was permeability P, which is related to the diffusion

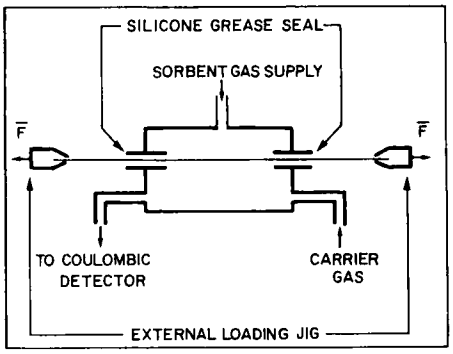

FIGURE 4 Cell for permeation studies on mechanically-loaded PET films.

coefficient (D) and solubility (S) by:

$$P = DS \tag{58}$$

Experimental procedure

A standard permeation apparatus manufactured by Modern Controls was used. A schematic of the permeation cell is given in Figure 4. The sorbent and carrier gas were both maintained at one atmosphere. Thus, the driving force for permeation was a partial pressure differential; not an absolute pressure differential. The films were loaded externally and sandwiched between the two elements of the permeation cell. Due to the absence of internal pressure, a barrier of silicon grease at the film-cell interface was sufficient to prevent any leakage. The PET films were mounted in the permeation cell under zero stress and oxygen was allowed to reach a steady state flux through the membrane. The films were then progressively stressed to higher levels; steady-state permeation was re-established at each level. Two types of PET films were studied: extruded and biaxially-oriented. The stretched films were produced at 100 C on a long film stretcher. Orientation was 4X by 2.8X.

In another experiment,[28] two-liter PET bottles (oriented 4X by 2.8X upon blowing) were pressurized with carbon dioxide. The bottles were capped with a gage/valve assembly and pressurized. The sorbents studied were carbon dioxide and water, *i.e.*, not necessarily the pressurizing gas. A permeability value was calculated from the sorbent flux, the internal pressure and the average bottle thickness. The bottles were assumed to be cylindrical and stresses were calculated using thin-wall-vessel theory. Thin-wall-vessel theory assumes that the radial stress can be neglected. This treatment was justified here because the wall-thickness-to-radius ratio was very small: $5.5\,10^{-3}$. All the data reported in this section were collected at room temperature, by the authors of Reference 28.

Results and discussion

Evaluation of parameters B, f_g, β_f and γ in the case of amorphous PET Since our constitutive equations have been derived in terms of the volumetric expansion

of the free volume, we need a stress-strain relationship in order to use the available permeability data reported as a function of the stress state. For a fully amorphous material, ε_{kk}^f is related to the hydrostatic stress σ_{kk} by:

$$\varepsilon_{kk}^f = \frac{\beta_f}{3}\sigma_{kk} \tag{59}$$

where β_f = compressibility of the free volume. (As explained earlier, the occupied volume in the sense of Turnbull is compressible). From References 13 and 30, we find that $f_g \simeq 0.033$ and we learn that for amorphous PET:

$$\frac{\beta_f}{\alpha} \simeq 0.36\ \text{cm}^2/\text{kg}$$

From Reference 30, $\alpha \simeq 1.6510^{-4}\,C^{-1}$. The above value for α was given for a semi-crystalline PET. Assuming α is unchanged for amorphous PET we have:

$$\beta_f = 0.6\ 10^{-5}\ \text{cm}^2/\text{kg}\ (4.17\ 10^{-7}\ \text{in}^2/\text{lb})$$

B can be evaluated from α and the WLF parameters C_1 and C_2 of the shift factor:

$$B = 2.303\alpha C_1 C_2 \tag{60}$$

Using the standard values for an amorphous polymer ($C_1 = 17.44$ and $C_2 = 51.6$) we find:

$$B = 0.34 \tag{61}$$

Since the penetrant molecules of interest are small, we will further make the assumption $B^D \simeq B$. The value of γ does not need to be calculated with accuracy in this analysis. It will be sufficient to know that it can be neglected for low activity penetrants.

The stress dependence of D and P in the glassy state Equation (27) can be rewritten as follows:

$$D = D_0 \exp\left[\frac{B^D}{f_g}\frac{\gamma C^N}{f_g + \varepsilon_{kk}^f + \gamma C^N}\right]\exp\left[\frac{B^D}{f_g}\frac{\varepsilon_{kk}^f}{f_g + \varepsilon_{kk}^f + \gamma C^N}\right] \tag{62}$$

Since the penetrants of interest (O_2, CO_2 and H_2O) have a low activity in PET, swelling is minimal and the following approximation is valid:

$$\gamma C^N \ll f_g$$

Furthermore, for low strain levels, we also have:

$$\varepsilon_{kk}^f \ll f_g$$

Therefore, expression (62) may be rewritten as:

$$D \simeq D_0 \exp\left(\frac{B^D}{f_g^2}\varepsilon_{kk}^f\right) \tag{63}$$

At low strain levels, then:

$$D \simeq D_0\left(1 + \frac{B^D}{f_g^2}\varepsilon_{kk}^f\right) \tag{64}$$

Combining expressions (59) and (63) and differentiating gives the relative change in diffusivity due to an externally applied load:

$$\frac{\Delta D}{D} = \frac{B^D}{f_g^2}\frac{\beta_f}{3}\sigma_{kk} \tag{65}$$

If the Hildebrand–Peterlin theory is obeyed, S is a much weaker function of σ_{kk} than D (See the section on solubility in Part I). By differentiating expression (58) we find that the relative change in permeability is dominated by the change in diffusivity:

$$\frac{\Delta P}{P} = \frac{B^D}{f_g^2}\frac{\beta_f}{3}\sigma_{kk} \tag{66}$$

Expressions (65) and (66) are valid for small stresses only. They predict the **initial** variation of P and D due to an externally applied load.

Correction for crystallinity As a first approximation, the following correction can be used for semi-crystalline polymers:[25]

$$D = D_a(1 - X_c) \tag{67}$$

or:

$$P = P_a(1 - 2X_c + X_c^2) \tag{68}$$

where: P_a and D_a are the permeability and diffusivity for the amorphous phase and X_c is the degree of crystallinity. The above correction accounts for the fact that the amorphous phase dominates transport properties. Note that this correction does not appear in the relative changes $\frac{\Delta D}{D}$ or $\frac{\Delta P}{P}$ as long as the degree of crystallinity is uniform both spatially and in time. A more important correction must be made, however: In a semi-crystalline polymer, the stress experienced by the amorphous phase is smaller than that experienced by the material as a whole. This is due to the fact that (1) the amorphous regions have a higher compressibility than the crystalline regions and (2) displacement continuity at the interface between the amorphous phase and crystalline phase must be satisfied.[25] Therefore (66) must be modified slightly by introducing the ratio ϕ of the effective stress (experienced by the amorphous region) to the externally applied stress:

$$\frac{\Delta P}{P} = \phi\frac{B^D}{f_g^2}\frac{\beta_f}{3}\sigma_{kk} \tag{69}$$

The morphology of a semi-crystalline polymer depends on the circumstances of crystallization and subsequent thermal and mechanical treatment.[13] As a result, ϕ is expected to be a strong function of the specimen thermal and mechanical history, making predictions of ϕ nearly impossible. We will now check the agreement of expression (69) with experimental data borrowed from Reference 28. These data show the dependence on stress of the permeability of PET to O_2, CO_2 and H_2O.

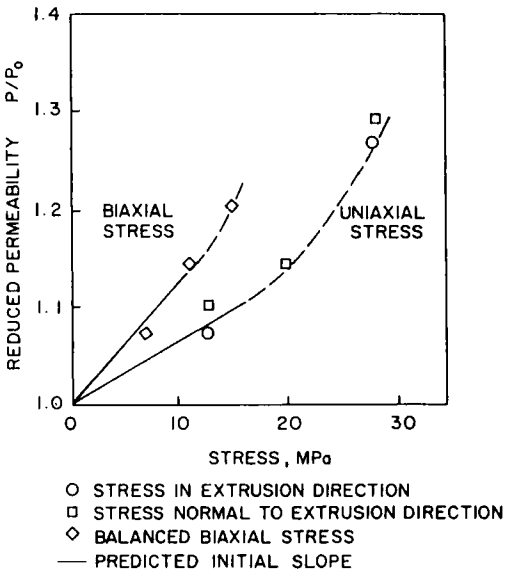

FIGURE 5 Stress dependence of permeability; oxygen in extruded PET.[28]

The case of extruded PET The extruded PET studied was slightly crystalline: 4%. This will allow us to verify expression (69) for quasi-amorphous PET, *i.e.*, $\phi \simeq 1$. The experimental data are summarized in Figure 5. Two cases were studied: a balanced biaxial stress state and a uniaxial stress state. Permeability was found to be independent of the direction of the applied stress, indicating that the extruded films were isotropic. For a biaxial and uniaxial stress, $\sigma_{kk} = 2\sigma$ and $\sigma_{kk} = \sigma$, respectively. For a balanced biaxial stress state, the initial permeability changes for amorphous PET can then be predicted by:

$$\frac{\Delta P}{P} = 2\frac{B^D}{f_g^2}\frac{\beta_f}{3}\sigma \tag{70}$$

and similarly, for a unixial stress state:

$$\frac{\Delta P}{P} = \frac{B^D}{f_g^2}\frac{\beta_f}{3}\sigma \tag{71}$$

Expression (70) gives: $\frac{\Delta P}{P\sigma} = 12.6\,\text{Gpa}^{-1}$ $(8.7 \times 10^{-5}\,\text{psi}^{-1})$ and expression (71) gives $\frac{\Delta P}{P\sigma} = 6.3\,\text{GPa}^{-1}$ $(4.4 \times 10^{-5}\,\text{psi}^{-1})$. Figure 5 shows that the agreement with experimental data is remarkable. The doubling of the initial slope from uniaxial to biaxial stress states is a good check of the proposed free-volume-based model. Examination of (62) suggests that the permeability should increase more slowly at higher stresses. This is not borne out of Figure 5 (see broken lines). A simple

calculation will reveal that reduction of the cross-sectional area of the polymer upon stretching is far too small to explain the observed upward deviation merely by the fact that the true stress becomes higher than the engineering stress. Thus, the upward inflection is perhaps indicative of damage formation or morphology changes.

The case of oriented PET As indicated earlier, permeability tests were also conducted on biaxially oriented PET. The main differences in transport properties with extruded PET are related to the higher degree of crystallinity, resulting in a lower value of ϕ (A degree of crystallinity of 28% was reported for the oriented PET studied in this section). ϕ was evaluated on semicrystalline PET by the authors of Reference 30. A value of 0.694 was reported but, unfortunately, this cannot be reused for specimens which experienced a different thermal and mechanical history. Since the available data points for oriented PET were obtained from pressurized cylinders, we have $\sigma_{kk} = 1.5\sigma_h$, where σ_h is the hoop stress.

It is found that, in order to obtain a good fit of the linear portion of the experimental data points, ϕ must be close to 0.46. Results pertaining to oriented PET are summarized in Figure 6. Our value of ϕ suggests a different crystalline morphology from that in the sample studied by the authors of Reference 30. As with amorphous PET, the broken line in Figure 6 cannot be fitted with the proposed theory.

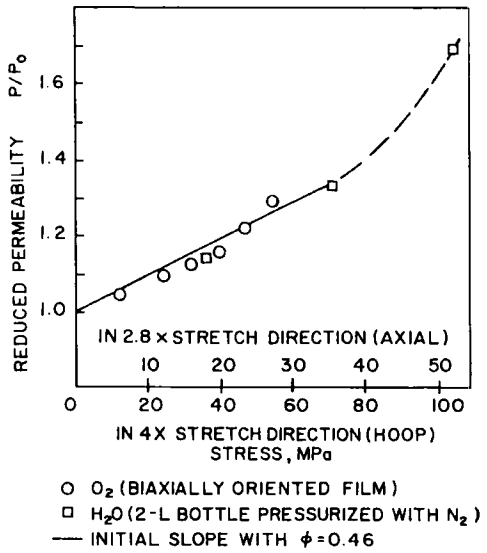

FIGURE 6 Effect of a biaxial stress on permeability; oxygen and water in oriented PET.[28]

Summary

Our findings on the stress dependence of D and P can be summarized as follows:

1. The free volume approach can predict the initial stress-induced variation of the permeability of an amorphous, glassy polymer. The slope prediction for amorphous PET is excellent.
2. The doubling of the slope from a uniaxial stress state to a biaxial stress state constitutes a good check of the free volume concept.
3. A correction can be made to account for the degree of crystallinity. This is due to the fact that the volumetric stress level experienced by the amorphous phase (dominating transport properties) is smaller than that experienced by the material as a whole. Unfortunately, ϕ is difficult to predict, due to a complex dependence on the thermal and mechanical history of the sample.
4. Expression (65) reveals an interesting property of polymers:
   Materials with a low diffusivity (*i.e.* a low f_g) will be more sensitive to stress because $\frac{\Delta D}{D}$ is inversely proportional to f_g^2.

THE STRAIN DEPENDENCE OF DIFFUSIVITY IN A THERMOPLASTIC POLY(IMIDE)

Experimental procedure

The polymer selected for this study was an amorphous thermoplastic poly(etherimide) with the commercial name of Ultem[31] 1000® ($T_g = 217$ C). The measurement method used was sorption. The classical sorption experiment features a plane sorbate sheet of known thickness, suspended in an atmosphere maintained at constant temperature and at constant pressure. Mass uptake is plotted as a function of square root of time, and D is extracted from the initial slope. In our study, sample geometries were designed to permit deformation of the polymer in tension, compression, or shear while simultaneously monitoring small weight changes. This was accomplished by using a plastically-deformable substrate as a light-weight loading fixture. The arrangement for the sorption cell was an adaptation of the McBain apparatus.[6] In order to avoid periodic removal of the sample from the sorption cell, the sample was suspended directly from a digital balance by a nylon wire. Relative humidity was controlled by circulating moist air originating from a vapor exchanger containing a saturated salt solution. For optimal temperature control, the sorption cell and vapor exchanger were both kept immersed in a thermostated water bath. The digital balance was a Sartorius 1800 with a precision of 0.1 mg and with a serial I/O port which was used for real time data acquisition. A schematic of the set-up is given in Figure 7. The tests were conducted at 60 C and at a relative humidity of 87%, generated by

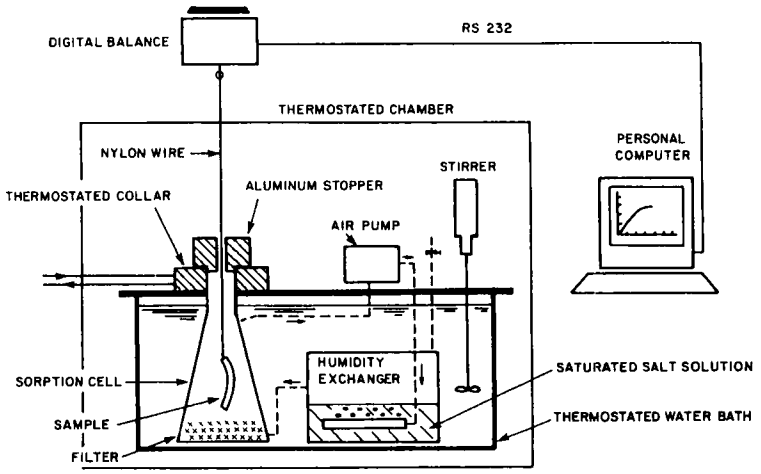

FIGURE 7 Modified sorption apparatus; note the beam specimen inside the sorption cell.

a sodium chloride solution. (Early tests of the apparatus showed that a 100% RH produces condensation on the specimen during small temperature fluctuations).

Specimen preparation

Ultem 1000 was selected for four main reasons: (1) its excellent adhesion to aluminum made it attractive for the kind of specimen geometry used, (2) its thermoplastic nature facilitates the interpretation of the results in light of the Free Volume Theory, (3) the relatively high diffusion coefficient of water in Ultem 1000 permits rapid data collection (D in Ultem is roughly 10 times higher than in an epoxy), and (4) stress relaxation is not a concern within the time frame of the tests, due to the large temperature gap between the test temperature (60 C) and T_g (217 C). In order to obtain tensile or compressive strains, Ultem films were bonded to the surface of rectangular aluminum beams (Al 6061) and the beams were then plastically deformed to the desired residual curvature with a four-point-bending fixture. (The beam substrate concept was originally proposed by Putter[32]). Beam curvature was uniform between the two central loading points and could yield residual longitudinal strain values on the outer skin, as high as 3.5%, in either a tensile or compressive mode. At this point, it is important to note that although the largest residual strains obtained in this study were well below the 7–8% tensile elongation yield limit of Ultem 1000,[31] our calculations indicate that the yield strain of Ultem 1000 could have been exceeded during the deformation operation in some cases. This is simply due to the fact that the recoverable elastic component of the beam deformation typically is four times as large as the plastic component. Thus, the lowest residual strain which may have been associated with prior plastic yield was estimated to be around 1.5%. Following the bending procedure, the extremities of the beam with non-uniform

curvatures were cut off. The specimen dimensions were the product of a compromise between the following requirements: (1) an upper limit on specimen weight was imposed by the capacity of the balance used (100 g in our case), (2) the largest possible beam thickness was desirable in order to minimize beam deflections and lower the experimental error on strain, (3) the film thickness had to be small compared to the beam thickness, in order to produce a uniform through-the thickness strain distribution and in order to limit test duration, and (4) the weight of the film had to be large enough so that the mass gain would not be too small compared to the weight range of the balance. The beam thickness and film thickness were 12.7 mm and 0.38 mm respectively. The specimen width was 25.4 mm. The aluminum substrate was vapor degreased, grit blasted, FPL-etched, and primed with a solution of Ultem 1000 in methylene chloride (5 g of Ultem per 100 ml). The film was bonded by compression molding at 250 C and 14 Mpa (2000 psi) in a hot press. This bonding procedure produced a polymer-to-metal bond of sufficient quality to withstand large deformations as well as environmental attack for the duration of the test. Note that for small strains, an **elastic** deformation was produced in the film. This can be explained by the fact that stress relaxation was minimal in the time frame of the sorption tests (one day for a thickness of 0.38 mm). Finally, all the specimens were conditioned in a vacuum oven at 60 C, for three days, prior to plastic deformation and testing.

In order to obtain a shear strain state, samples were made consisting of a solid aluminum cylinder coated with a thin poly(imide) film of uniform thickness. This was accomplished by molding a square block of Ultem 1000 around the cylinder, which was then machined down with a lathe with a tolerance of $\pm 25\ \mu$m. The cylinders were then plastically deformed in a torsional jig, thereby producing a quasi-uniform shear strain in the film bonded to their outer skin. The design requirements, surface treatments and bonding technique were the same as with the beam specimens. The cylinder diameter and film thickness were 12.6 mm and 0.5 mm respectively. Shear strains as large as 4% could be obtained. All the torsional specimens were conditioned in a vacuum oven at 60 C for five days, prior to plastic deformation and testing.

The bonding procedures for the polymer layers onto the aluminum substrates resulted in residual thermal stresses. Since our goal was to measure the **relative** change in diffusivity and solubility upon straining, the absolute value of the initial diffusivity and solubility (*i.e.*, with zero mechanical strain) were not needed as long as they remained the same for all the specimens used for one curve. For this reason, great care was taken during the fabrication process to reproduce the same temperature history on all specimens. By keeping the reference stress state uniform, this method eliminated the need to calculate the residual stresses.

Results and discussion

A typical sorption curve obtained from our tests is shown in Figure 8. The initial mass gain was not linear when plotted against time but became linear when plotted against square root of time. Figure 9 illustrates this result by showing a

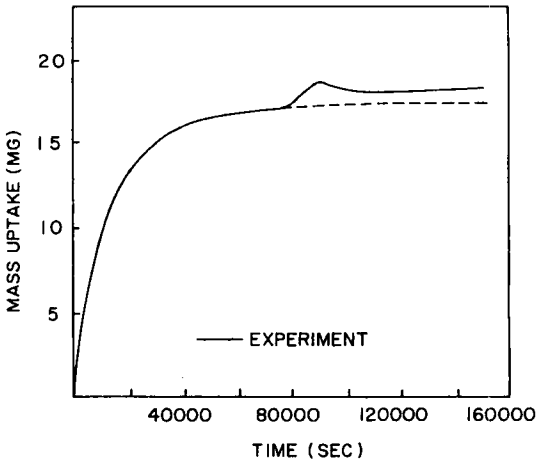

FIGURE 8 Sorption curve for a torsional specimen; the Ultem 1000 film is subjected to a shear strain level of 0.83%. (60 C).

plot of the fractional weight increase (multiplied by a factor of two), against the square root of time normalized to the film thickness. The straight line up to 70% of the saturation level is indicative of Fickian behavior with a constant diffusion coefficient. The factor of two on the ordinate axis originates from the fact that only one side of the film is exposed to water vapor. Since initial moisture penetration proceeds as in a semi-infinite medium, the initial rate of mass uptake was half of what it would have been in a free film. The correction factor simply

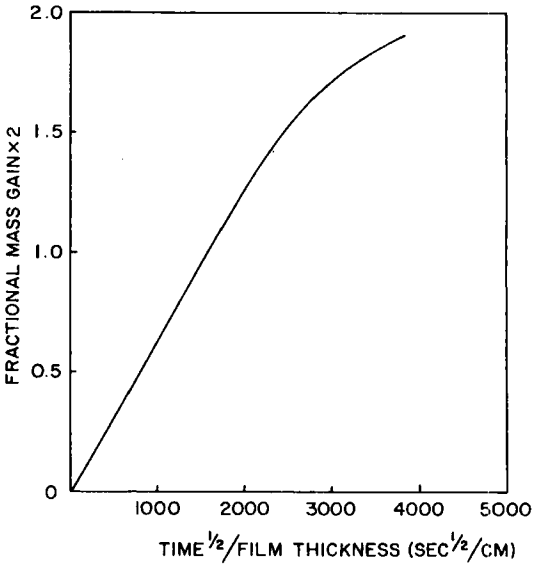

FIGURE 9 Normalized sorption curve; same specimen and same conditions as in Figure 8.

enabled us to extract the diffusion coefficient by measuring the initial slope according to the classical procedure.

Further examination of Figure 8 reveals that, as the maximum mass is approached, a departure from ideal Fickian behavior occurs, in the form of a sudden excess sorption. The excess mass was consistently observed on most specimens. Since this effect is also observed on neat films, it must be related to some kind of bulk viscoelastic response of Ultem. The exact nature of the mechanism involved is still unknown at this stage. It is fortunate that this relaxation phenomenon did not come into play at an earlier stage of sorption, when it would have most likely given rise to a non-Fickian kinetics. The dashed line in Figure 8 represents the extrapolated Fickian sorption. Since the anomalous behavior is transient and short, the extrapolated asymptote, and not the actual maximum, was used for the determination of the solubility of water vapor in Ultem.

Figure 10 shows the diffusion coefficient of water in Ultem, normalized to its value at zero strain, *versus* the longitudinal component of the strain (on the outer skin of a plastically bent beam). Positive, as well as negative, strain values are plotted. For small strains, a linear response, consistent with our theoretical predictions for an amorphous polymer in the elastic range can be seen. Note that the compressive strain state lowers diffusivity, whereas the tensile stress state increases diffusivity, as expected. Further, whenever the longitudinal strain exceeds 1% in absolute value (*i.e.*, in compression or in tension), a slope reversal occurs. These nonlinear portions of the diffusivity-strain behavior are shown with broken lines on Figure 10. A very large decrease in D at high tensile elongations,

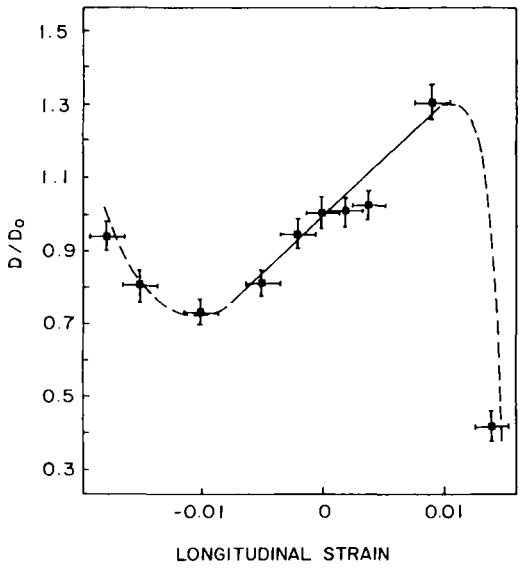

FIGURE 10 Effect of strain in the water vapor-Ultem 1000 system; normalized diffusivity in a film subjected to a uniaxial strain (beam specimens, 60 C).

similar to what we encountered in our study, has been reported in polyethylene drawn at 60 C and tested at 25 C. The sharp drop was attributed to orientation-induced crystallization.[25] Because of the lack of symmetry in Ultem's molecular chains, however, this mechanism is unlikely to have occurred here. As for the increase of D at large compressive strains, damage growth appears to be a plausible explanation at first, since defects are known to enhance the transport rate in polymers.[7] However, no damage could be detected visually in any of the specimens. Moreover, if damage growth was involved, the same behavior would be seen in tension, more pronounced and earlier. At this point, it is instructive to recall that because of the large strains needed to deform the beam permanently plastic deformation is likely to have developed in the specimens featuring a residual surface longitudinal strain as low as 1.5%, which is precisely the strain level at which we see our theoretical predictions fail. The precise molecular events which could lead to such an abrupt change in diffusion behavior under plastic deformation are not known by the authors at this time.

Recalling that the compressibility of the free volume is roughly one-half of that of the specific volume, the initial slope in Figure 10 can be related to a slope with respect to the dilatational strain of the free volume, by the following approximation:

$$\frac{\Delta D}{D_0 \varepsilon_{kk}^f} = \frac{\Delta D}{D_0 \varepsilon_{xx}} \frac{2}{(1 - \nu_1 - \nu_2)} \tag{72}$$

with: ν_1 = lateral Poisson's ratio (plastic deformation of the beam)
ν_2 = Poisson's ratio of the polymer

Poisson's ratio ν_1 was approximated by the value 0.5 because the residual deformation in the beam (after unloading the bending fixture) is dominated by the plastic component of strain, and plastic flow is known to occur with no volume change. Poisson's ratio ν_2 was reported[33] to be 0.435. Once multiplied by the correction factor introduced in expression (72), the experimentally measured slope for small strains (in Figure 10), was found to be equal to 1230 (dimensionless). According to the Free Volume Theory, this value must be equal to $\frac{B^D}{f_g^2}$. If B^D is assumed to be equal to 0.4, a f_g equal to 0.018 is found. If B^D is assumed to be equal to 1.0, a f_g equal to 0.029 is found. (0.4 to 1 is the range for B suggested in the literature[13]). Noting that these two values are close to the lower and upper limits quoted for f_g in the literature,[13] we conclude that expression (64) is obeyed at low strain levels and that the assumption that the stress dependence of D below T_g is free volume governed, is verified.

Figure 11 shows the diffusion coefficient of water vapor in Ultem, normalized to its value at zero strain, *versus* shear strain (on the skin of a plastically twisted cylinder). The Lagrangian definition of strain is used. Diffusivity is found to be independent of the level of shear strain. Since a pure shear strain state does not alter the specific volume of the material, the above result constitutes a crucial verification of the Free Volume Theory.

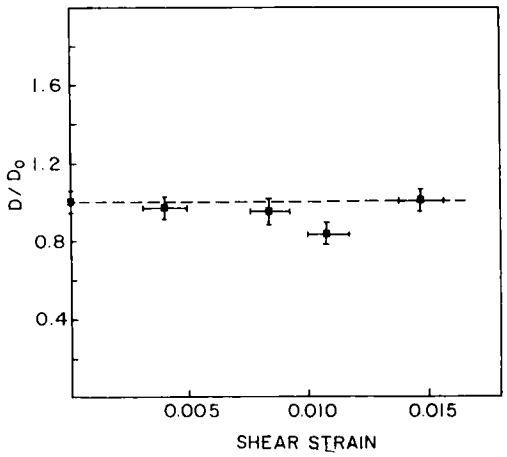

FIGURE 11 Effect of strain in the vapor-Ultem 1000 system; normalized diffusivity in a film subjected to a shear strain. (Torsional specimens, 60 C).

Summary

Our findings on the strain dependence of D can be summarized as follows:

1. Expression (64) can predict the initial strain-induced variation of diffusivity in the water-Ultem system, both under a tensile stress state and a compressive stress state.
2. The initial reduction of D under a compressive stress state constitutes an excellent check of the free volume concept.
3. Shear strain does not affect D.

THE STRAIN DEPENDENCE OF SOLUBILITY IN LOW DENSITY POLY(ETHYLENE) AND IN A THERMOPLASTIC POLY(IMIDE)

The case of carbon dioxide in low density poly(ethylene)

A behavior consistent with the theories proposed in Part I has been reported in Reference 25, where the authors studied the permeation of CO_2 in low density poly(ethylene) films under strain (see Figure 12). For small strains, expression (51) is able to describe the behavior correctly **within the experimental error**. The main result is the confirmation that solubility is fairly insensitive to low strains. Practically, this means that if a polymer-penetrant system exhibiting similar behavior was encountered in a durability study, the solubility could easily be assumed to be stress independent. For large strains, expression (51) also leads to correct predictions[25] (See Figure 12), but it is difficult to lend any significance to this result in view of the fact that crystallinity appears, leading to properties which cannot be adequately described by an unmodified free volume theory. It was also

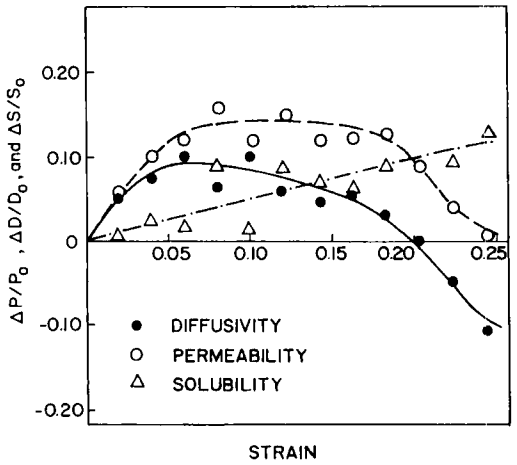

FIGURE 12 Effect of strain in the carbon dioxide-low density PE system; normalized D, S, and P *vs.* undirectional strain.[25]

shown in Part I that diffusivity is much more sensitive to strain than solubility, roughly by an order of magnitude; this is also quite evident in the small-strain portion of the experimental data presented in Figure 12. We conclude that the solubility models based on the thermodynamics-of-mixtures approach and the free-volume-occupation approach seem to work reasonably well at low strains for the poly(ethylene)-carbon dioxide system. The fact that one finds agreement below T_g, where thermodynamic equilibrium is not achieved, is not too surprising when one considers that the derivations were based primarily on geometric considerations (either lattice theory or free volume occupancy).

The case of water vapor in Ultem 1000 poly(imide)

The solubility data discussed in this section were collected along with the diffusivity data presented in Figures 10 and 11. The same specimens and the same conditions were used. Figure 13 shows the relative change of the solubility of water in Ultem films subjected to varying levels of longitudinal strains. Re-using expression (72), and replacing D by S, yields a slope with respect to the dilatation of the free volume equal to 1077 (dimensionless), which is roughly the slope we found for the diffusion coefficient. According to expression (51), this slope should be close to 40. The reason behind this sharp departure from the theory could be related to the fact that the hydrogen bond network of the poly(imide) is gradually broken up under strain, thereby releasing an increasing number of hydrogen bond sites for water. Unfortunately, this explanation is not consistent with our data for S under a shear strain. Figure 14 shows the relative change of the solubility of water in Ultem films subjected to varying levels of shear strains. As in the case of diffusivity, solubility is found to be independent of the level of shear strain. This result was expected, since a pure shear strain state does not change the specific

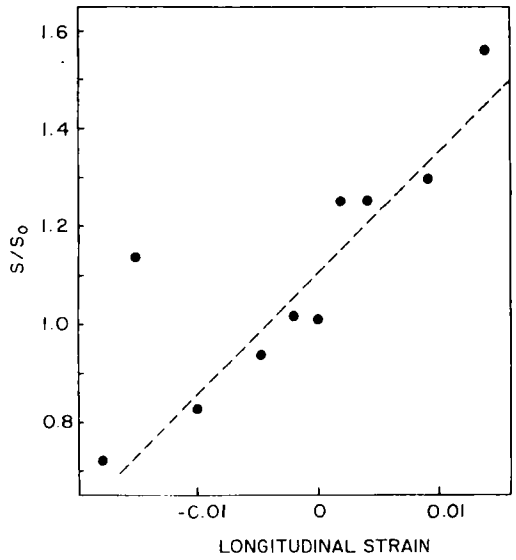

FIGURE 13 Effect of strain in the water vapor-Ultem 1000 system; normalized solubility in a film subjected to a biaxial strain. (Beam specimens, 60 C).

volume of the material; however, it is not consistent with the hydrogen bond argument developed above because hydrogen bonds would also be broken up under shear. Finally, it should be noted that for highly oriented (extruded or calendered) polymers, the argument on behalf of no volume change in pure shear may not apply.

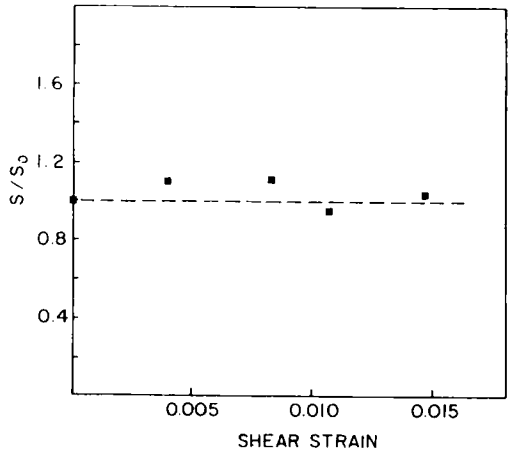

FIGURE 14 Effect of strain in the water vapor-Ultem 1000 system; normalized solubility in a film subjected to a shear strain. (Torsional specimens, 60 C).

Summary

1. Expression (51) in Part I can predict the initial variation of solubility under a uniaxial strain in the carbon dioxide-low density PE system but not in the water-Ultem system.
2. A shear strain state does not affect solubility in the water-Ultem system, as expected.

CONCLUSION

With the exception of the strain dependence of solubility in Ultem 1000, good agreement has been found between the theory and experiment at small strain levels. This leads us to conclude that the models presented in Part I hold very promising predictive capabilities for joint durability studies. The lack of agreement with the solubility model for certain materials can be easily remedied, simply by replacing expression (51) in Part I by an equation determined empirically. Such a procedure is perfectly legitimate in the framework of an engineering solution of the durability problem.

Thus, far, the data were mainly a description of the short term response of the polymer. Our level of confidence is now sufficient to embark on more complex simulations, including the viscoelastic behavior of the polymer over longer times. Part III will include a validation problem featuring a time-dependent diffusion coefficient, as well as numerical simulations of moisture penetration in a butt joint.

NOTATION

D: Diffusion coefficient
D_0: Diffusion coefficient in the reference state
T: Temperature
T_0: Reference temperature
f_0: Reference fractional free volume of the polymer
α: Coefficient of thermal expansion of the free volume
B^D: Parameter inversely related to the critical void size
γ: Coefficient of expansion due to moisture sorption
C: Penetrant concentration
g: Subscript referring to the glass transition temperature as the reference state
S: Solubility
S_a: Solubility of the amorphous phase (semicrystalline polymer)
P: Permeability
P_a: Permeability of the amorphous phase (semicrystalline polymer)
ε_{kk}: Dilatational strain
ε^f_{kk}: Dilatation of the free volume

σ_{kk}: Dilatational stress
σ: Uniaxial stress
β_f: Compressibility of the free volume
X_c: Degree of crystallinity
Φ: Ratio of the effective stress to the externally-applied stress (semicrystalline polymer)
ν_1: Poisson's ratio for aluminum
ν_2: Poisson's ratio for Ultem 1000

References

1. Y. Weitsman, *J. Mech. Phys. Solids* **35,** 73 (1987).
2. M. Tirrell and M. F. Malone, *J. Polym. Sci. Polym. Physics Ed.* **15,** 1569 (1977).
3. J. Crank, *The Mathematics of Diffusion,* 1*st. Ed.* (Oxford at the Clarendon Press, London, 1956).
4. H. L. Frisch, T. T. Wang and T. K. Kwei, *J. Polym. Sci.* **A-2,** Vol 7, 879 (1969).
5. N. L. Thomas and A. H. Windle, *Polymer* **23,** 529 (1982).
6. R. M. Felder and G. S. Huvard, *Methods of Experimental Physics,* Vol. 16, R. A. Fava, Ed. (Academic Press, New York, 1980), Chap 17, pp. 315–377.
7. J. Comyn, *Polymer Permeability* (Elsevier Applied Science Publishers, London and New York, 1985), Chap. 2–3, pp. 11–117.
8. F. A. Long and D. Richmond, *J. American Chem. Soc.* **82,** 513 (1960).
9. P. Neogi, M. Kim and Y. Yang, *AICHE Journal* **32,** 1146 (1986).
10. D. Turnbull and M. H. Cohen, *J. Chem. Phys.* **34,** 120 (1961).
11. M. H. Cohen and D. Turnbull, *ibid.* **31,** 1164 (1953).
12. P. B. Macedo and T. A. Litovitz, *ibid.* **48,** 845 (1965).
13. J. D. Ferry, *Viscoelastic Properties of Polymers,* 3rd. Ed. (John Wiley and Sons Inc., New York, 1980).
14. J. S. Vrentas, J. L. Duda, H. C. Ling and A. C. Jau, *J. Polym. Sci., Polym. Phys. Ed.* **23,** 289 (1985).
15. J. H. Noggle, *Physical Chemistry* (Little, Brown and Company, Boston, 1985), Chap. 9, pp 445–449.
16. W. G. Knauss and J. J. Emri, *Composites and Structures* **13,** 123 (1981).
17. S. Matsuoka, G. H. Frederickson and G. E. Johnson, *Lecture Notes in Physics 277, Molecular Dynamics and Relaxation Phenomena in Glasses,* T. Dorfmuller and G. Williams, Eds. (Springer-Verlag, Berlin, 1985), p. 188–202.
18. L. C. E. Struik, *Physical Aging in Amorphous Polymers and Other Materials* (Elsevier, Amsterdam, 1978), Chap. 10, pp. 125–134.
19. M. J. Adamson, *Some Free Volume Concepts of the Effects of Absorbed Moisture on Graphite/Epoxy Composite Laminates,* in Adhesion Science Review, Vol. 1, H. F. Brinson, J. P. Wightman and T. C. Ward, Eds. (Commonwealth Press, Inc., Richmond, Virginia, 1987), pp. 87–101.
20. A. Cochardt, G. Shoeck and H. Wiedersich, *Acta Metallogr.* **3,** 533 (1955).
21. F. S. Ham, *J. Appl. Phys.* **30,** 915 (1959).
22. G. Akay, *Polym. Engg. and Sci.,* **22,** 798 (1982).
23. P. J. Flory, *Principles of Polymer Chemistry* (Cornell University Press, Ithaca, 1983), pp. 495–440.
24. A. Peterlin, *J. Macromol. Sci. Physics,* **B11,** 57 (1975).
25. H. Yasuda and A. Peterlin, *J. Appl. Polym. Sci.* **18,** 531 (1976).
26. J. C. Phillips and A. Peterlin, *Polym. Engg. and Sci.* **23,** 734 (1983).
27. J. S. Vrentas, J. L. Duda and Y. C. Ni, *J. Polym. Sci., Polym. Phys. Ed.* **15,** 2039 (1977).
28. R. W. Seymour and S. Weinhold, *Proceedings of Ryder Conference '85, Ninth International Conference on Oriented Plastic Containers,* p. 281 (1985).
29. L. H. Wang and R. S. Porter, *J. Polym. Sci., Polym. Phys. Ed.* **22,** 1645 (1984).
30. P. Zoller and P. Balli, *J. Macromol. Sci. Physics* **B18,** 555 (1980).
31. *Ultem Polyetherimide 1987 Property Guide,* GE Plastics, Ultem Products Operation, Pittsfield, MA, U.S.A.

32. S. Putter and S. Shimabukuro, *SM Report 87–10,* Grad. Aer. Labs., Cal Tech, Pasadena, CA, U.S.A., April 1987.
33. R. Brandes, *personal communication,* GE Plastics Division, Pittsfield, MA, U.S.A.
34. J. N. Reddy and S. Roy, *Report No. VPI-E-85.18,* Department of Engineering Science and Mechanics, VPI & SU, Blacksburg, VA, U.S.A. (1985).
35. S. Roy and J. N. Reddy, *Report No. VPI-E-86.28,* Department of Engineering Science and Mechanics, VPI & SU, Blacksburg, VA, U.S.A. (1986).
36. S. Roy, *PhD Dissertation,* VPI & SU, Blacksburg, VA, U.S.A. (1987).
37. G. Levita and T. L. Smith, *Polym. Engng. and Sci.* **21,** 936 (1981).
38. T. L. Smith, W. Opperman, A. H. Chan and G. Lenta, *Polymer Preprints* **24(1),** 83 (1983).
39. G. S. Springer, *Environmental Effects on Composite Materials, Vol. 2* (Technomic Publishing Company, Inc., 1984), pp. 15, 302.